Enhanced CO_2 Capture by Sorption on Electrospun Poly (Methyl Methacrylate)

Michele Ciulla, Valentino Canale, Rafal D. Wolicki, Serena Pilato, Pantaleone Bruni, Stefania Ferrari, Gabriella Siani, Antonella Fontana, Pietro Di Profio*

Department of Pharmacy, University of Chieti-Pescara "G. d'Annunzio", via dei Vestini, I-66100 Chieti (Italy)

*Corresponding Author: pietro.diprofio@unich.it

(A)

FTIR-ATR analysis

Methods

IR spectra were obtained using a Shimadzu IRAffinity-1S FTIR spectrophotometer (Shimadzu Italia S.r.l., Milan, Italy) equipped with a sealed and desiccated interferometer, a DLATGS (Deuterated Triglycine Sulphate Doped with L-Alanine) detector and a single reflection diamond ATR crystal (QATR 10, Shimadzu Italia S.r.l., Milan, Italy). All FTIR spectra were recorded in the range from 3250 to 450 cm^{-1} co-adding 45 interferograms at a resolution of 4 cm^{-1} with Happ–Genzel apodization. The ATR crystal was carefully cleaned before each analysis, a background was recorded for each sample and the measurements were performed in triplicate.

Spectra manipulation was carried out with the software LabSolution IR version 2.27 (Shimadzu Italia S.r.l., Milan, Italy). The software allowed to carry out a "purity test", by which the degree of matching between any pairs of data can be obtained. This purity, *P*, is given by the least-squares-fit coefficient calculated for every intensity pair of the two data being compared. This factor P can be calculated using the following formula:

$$P = \frac{\sum_{i}^{n} (s_i - \bar{s})(r_i - \bar{r})}{\sqrt{\sum_{i}^{n} (s_i - \bar{s})^2 \sum_{i}^{n} (r_i - \bar{r})^2}}$$

In this formula, s_i and r_i are the respective intensities for the same horizontal coordinate value, and n is the number of data points. $\bar{s}$ and $\bar{r}$ are the average intensities of each data. The purity value is between 0 and 1. "0" indicates no identity between the two data, and "1" indicates that the two data are identical.

A regression curve plot that indicates the purity match between the two data and also the calculation results is reported (Figs. S4-S8). The purity plots show the correlation curve of the intensities of source data with respect to those of reference data. Slope and intercept of the correlation curve are given in the text report. This test was used to evaluate differences in chemical composition between samples before and after adsorption (Figs. S4-S6), and also between amorphous and electrospun PMMAs (Figs. S7-S8).

Results

Pre- and post-adsorption comparisons

Figures S1-3 compare the FTIR spectra of each material before and after absorption in the range of 3250 – 450 cm^{-1}.

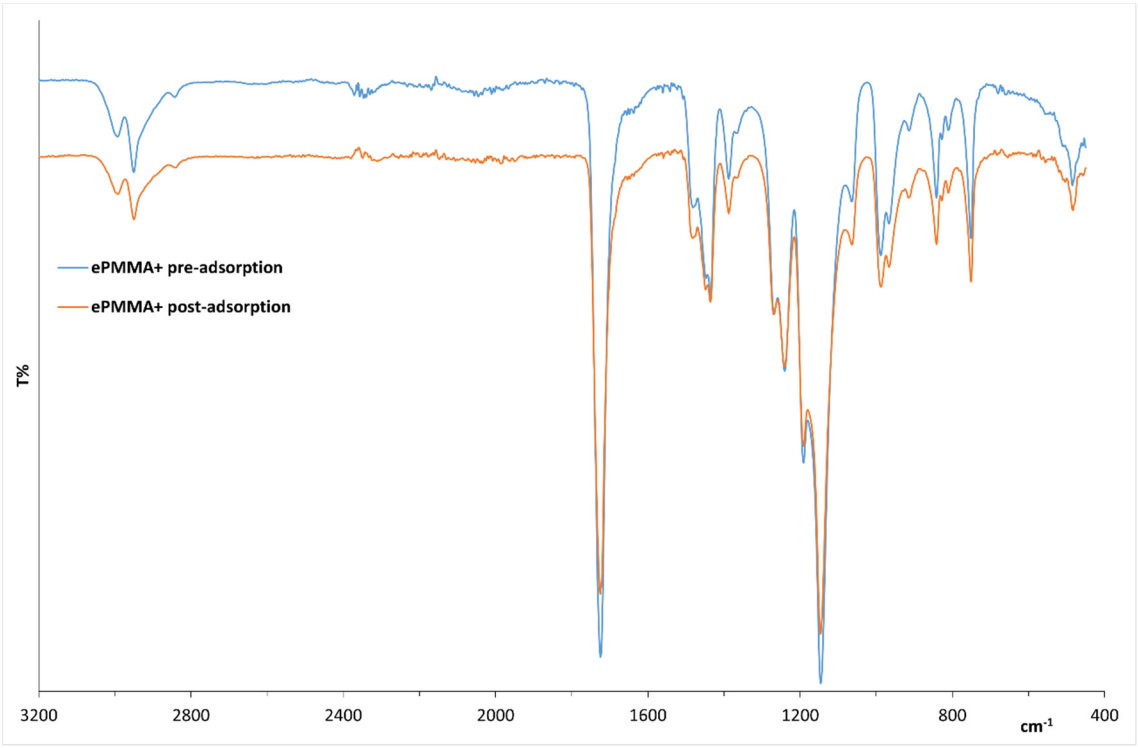

Figure S1. ATR-FTIR spectra comaprison of ePMMA+ pre- and post-adsorption.

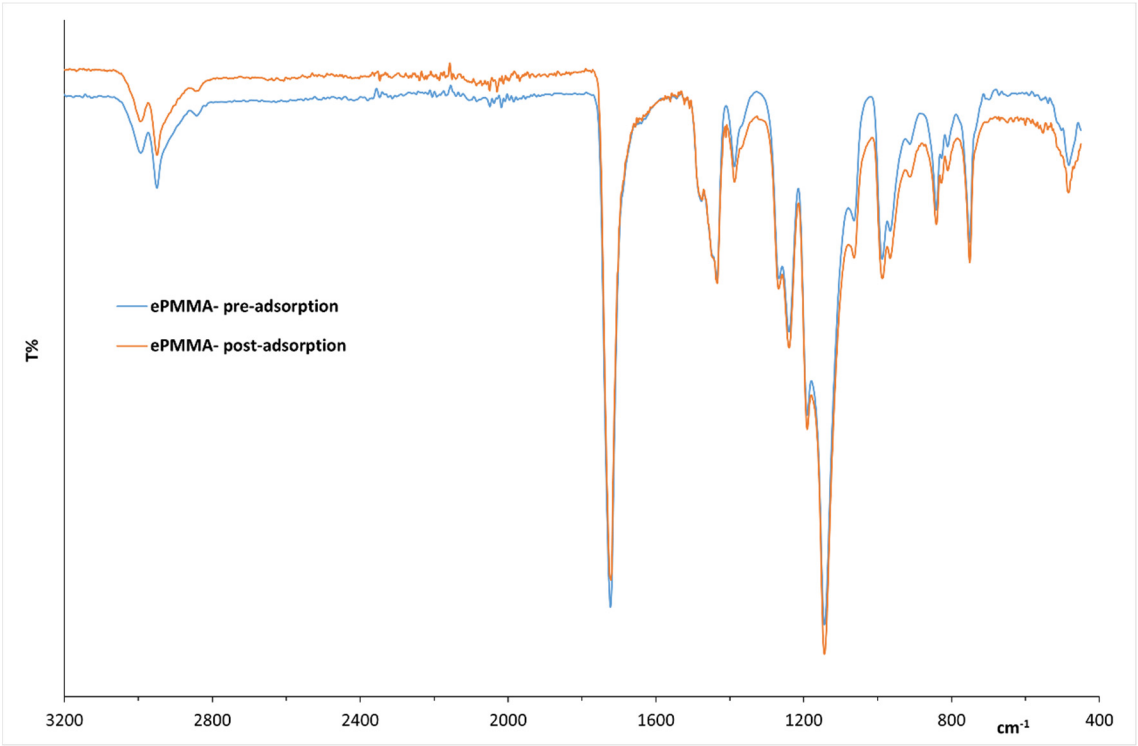

Figure S2. ATR-FTIR spectra comaprison of ePMMA- pre- and post-adsorption.

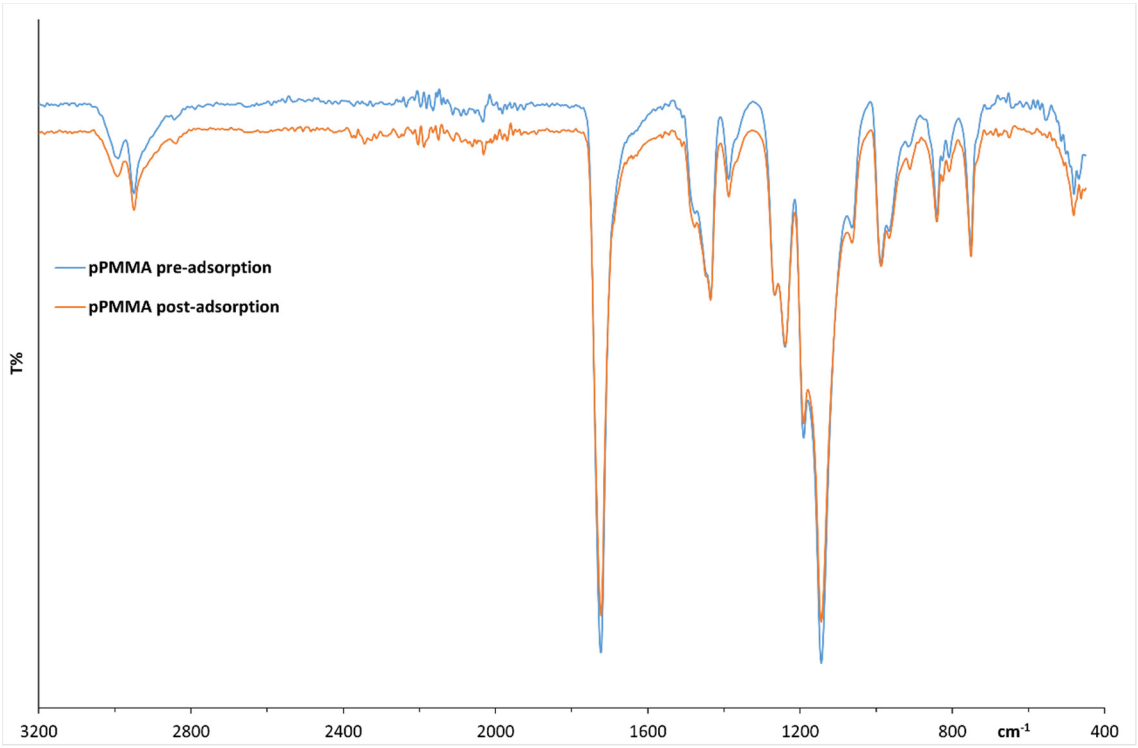

Figure S3. ATR-FTIR spectra comparison of pPMMA pre- and post-adsorption.

All spectra clearly present the typical PMMA features, in particular the C−H stretching modes of α-methyl, ester-methyl, and methylene groups at 2900−3000 cm^{-1} and the C-H bendings at 1350 – 1450 cm^{-1}; the C=O stretching at 1726 cm^{-1} and the three main bands in the 1350–1100 cm^{-1} region for ester group stretching vibrations. Notably, no chemical alterations are found, all peaks match before and after the sorption process.

The CO_2 peak around 2340 cm^{-1} is not visible in the post-adsorption spectra since the reduction of pressure to ambient conditions after opening the reactor, and placing the polymer upon the ATR, leading to a natural and quick release of the gas into the environment. This confirms the reversibility of the sorption, and an easy release of CO_2 from PMMA.

Purity index calculation

Based on the calculations shown in Figures S4-6 for each pair of samples, the purity index value was higher than 99% (small differences are due to the background noise and the possible background subtraction variations), confirming that although CO_2 leads to physical modifications, from a chemical point of view there is no evidence of alterations of the PMMA chains or functional groups.

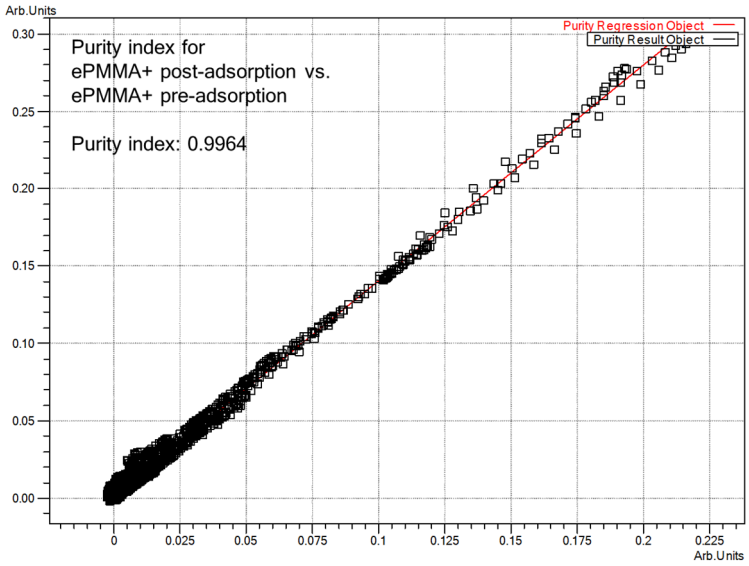

Figure S4. Purity index graph for ePMMA+ post-adsorption vs. ePMMA+ pre-adsorption.

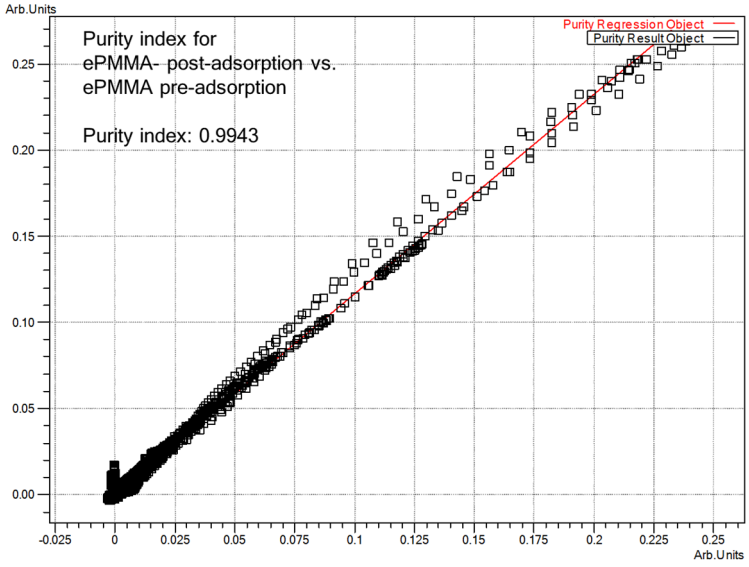

Figure S5. Purity index graph for ePMMA- post-adsorption vs. ePMMA- pre-adsorption.

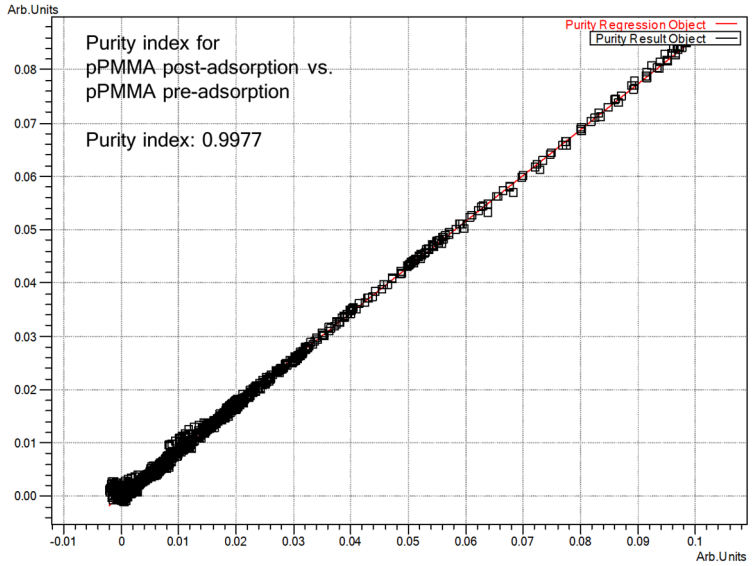

Figure S6. Purity index graph for pPMMA post-adsorption vs. pPMMA pre-adsorption.

The same procedure was carried out to evaluate any differences between the polymer and the electrospun-related materials (Figure S7-8). In this case, the sources for the purity index calculation were the electrospun PMMA and the reference was the FTIR spectrum of the amorphous powder. Results show no differences in the chemical vibrations for both the electrospun PMMA, with a purity index values higher than 99%.

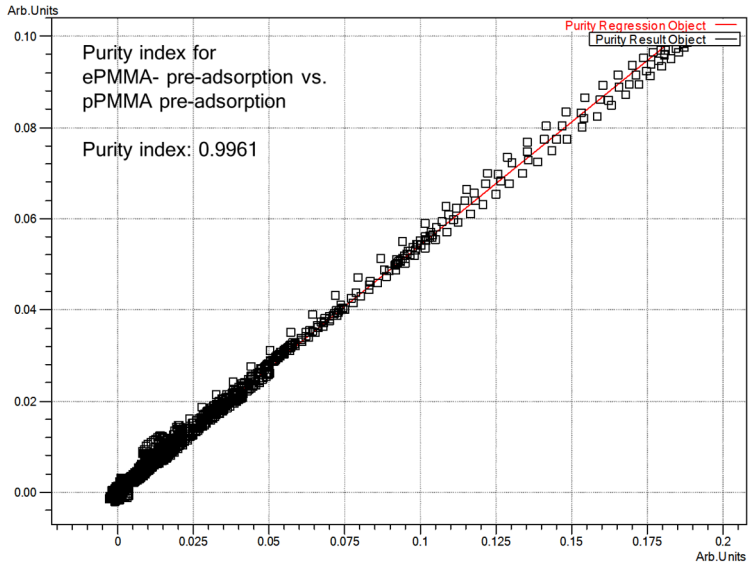

Figure S7. Purity index graph for ePMMA- and pPMMA pre-adsorption.

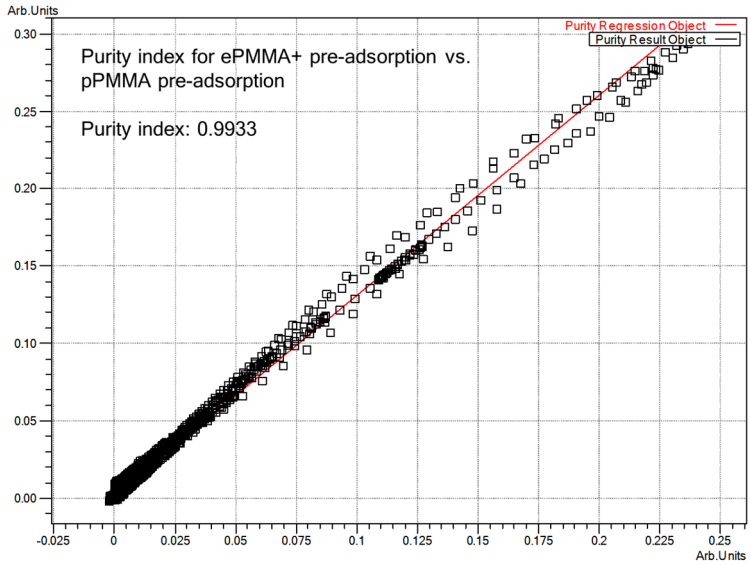

Figure S8. Purity index graph for ePMMA+ and pPMMA pre-adsorption.

(B)

CHARACTERIZATION OF THE EFFICIENCY LOSSES FOR PRISTINE AND REGENERATED ePMMAs

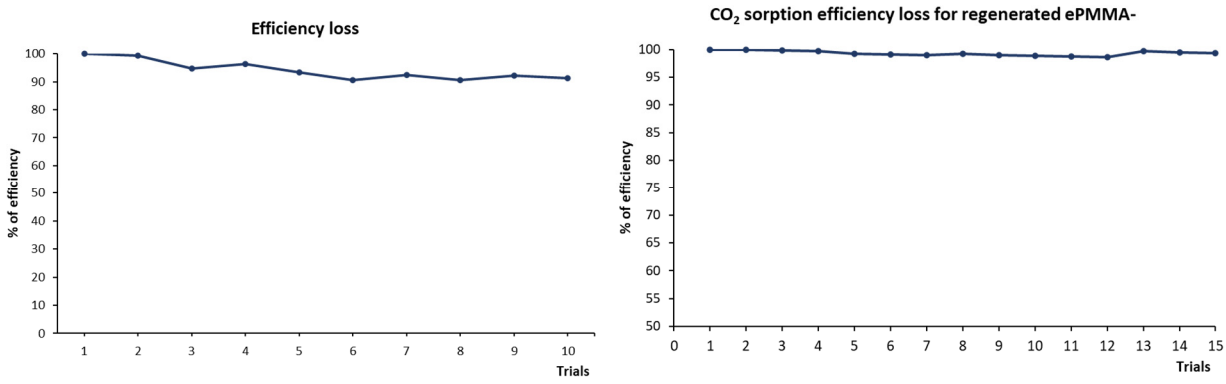

Figure S9, (a, left): CO_2 sorption efficiency loss for ePMMA- after 10 cycles of sorption/desorption at 20 °C/ 2 MPa; (b, right): CO_2 sorption efficiency loss for regenerated ePMMA- after 15 cycles of sorption/desorption at 20 °C/ 2 MPa.

(C)

COMPARISON OF CO_2 SATURATION TIMES FOR pPMMA and ePMMAs

Table S1: Average times for reaching 90% saturation of CO2 for selected PMMAs and P/T conditions, and comparison of ePMMAs to pPMMA

Types of PMMA	**Average time (sec) to reach 90% of total sorbed CO_2**	**Ratio ePMMA/powder**
pPMMA @ 40bar, 20°C	9.2	
pPMMA @ 30bar, 1°C	17.3	
ePMMA+ @ 40bar, 20°C	5.5	0.60
ePMMA+ @ 30bar, 1°C	7.0	0.40
ePMMA- @ 40bar, 20°C	7.0	0.98
ePMMA- @30bar, 1°C	5.2	0.30